Distribution Agreement

In presenting this thesis as a partial fulfillment of the requirements for a degree from Emory University, I hereby grant to Emory University and its agents the non-exclusive license to archive, make accessible, and display my thesis in whole or in part in all forms of media, now or hereafter now, including display on the World Wide Web. I understand that I may select some access restrictions as part of the online submission of this thesis. I retain all ownership rights to the copyright of the thesis. I also retain the right to use in future works (such as articles or books) all or part of this thesis.

Samia Khan March 30, 2023

The Effect of Two Experimental Treatments (R13 & Compound 11) on Sensory Axon Regeneration After Peripheral Nerve Injury

By

Samia Khan

Arthur W. English, Ph.D.
Adviser

Neuroscience and Behavioral Biology

Arthur W. English, Ph.D.
Adviser

Gillian Hue, Ph.D.
Committee Member

Jill Ward, Ph.D.
Committee Member

2023

The Effect of Two Experimental Treatments (R13 & Compound 11) on Sensory Axon Regeneration After Peripheral Nerve Injury

By

Samia Khan

Arthur W. English, Ph.D.
Adviser

An abstract of
a thesis submitted to the Faculty of Emory College of Arts and Sciences
of Emory University in partial fulfillment
of the requirements of the degree of
Bachelor of Science with Honors

Neuroscience and Behavioral Biology

2023

Abstract

The Effect of Two Experimental Treatments (R13 & Compound 11) on Sensory Axon Regeneration After Peripheral Nerve Injury

By Samia Khan

Recovery from peripheral nerve injuries (PNIs) is poor because axon regeneration is slow and inefficient. Experimental therapies that increase signaling of neuronal brain-derived neurotrophic factor (BDNF) through its TrkB receptor enhance axon regeneration, but treatments using recombinant human BDNF, or even the BDNF mimetic, 7,8-dihydroxyflavone (7,8-DHF), are not feasible because of their short biological half-life. A prodrug, R13, is metabolized in the liver and releases 7,8-DHF gradually. A target of BDNF-TrkB activation is the inhibition of asparagine endopeptidase (AEP), a lysosomal protease that can be inhibited by Compound 11 (CP11). The goals of this project were to compare the effects of treatments with R13 or CP11 on the regeneration of sensory axons following PNI and to evaluate the proportions of different classes of sensory (dorsal root ganglion, DRG) neurons that successfully reinnervate muscle targets following either treatment. We hypothesized that both treatments would result in enhanced regeneration of sensory axons, but the proportions of neurons expressing proteins associated with different classes of DRG neurons would not be changed. Following sciatic nerve transection and repair, C57BL/6J mice were treated for two weeks with either R13, CP11, or a control vehicle. Four weeks after injury, different fluorescent retrograde tracers were injected into the gastrocnemius (GAST) and tibialis anterior (TA) muscles to mark newly regenerated DRG neurons that had reinnervated these muscles. Using immunofluorescence, labeled DRG neurons expressing TrpV1, IB4, TH, VGLUT1, or multiple proteins were counted. Treatments with R13 or CP11 resulted in muscle reinnervation by twice as many DRG neurons as vehicle-treated controls, but neurons expressing proteins associated with different classes of DRG neurons were in roughly the same proportions. Both treatments are promising drug-based approaches to enhancing axon regeneration and function, and potentially, quality of life, for individuals living with PNI.

The Effect of Two Experimental Treatments (R13 & Compound 11) on Sensory Axon Regeneration After Peripheral Nerve Injury

By

Samia Khan

Arthur W. English, Ph.D.
Adviser

A thesis submitted to the Faculty of Emory College of Arts and Sciences
of Emory University in partial fulfillment
of the requirements of the degree of
Bachelor of Science with Honors

Neuroscience and Behavioral Biology

2023

Acknowledgements

I would like to acknowledge Dr. Arthur English for his invaluable guidance and mentorship throughout my time in his lab. I would also like to thank Dr. Robin Isaacson and Dr. Dario Carrasco for their advice and encouragement throughout my learning process in the English Lab, along with my committee members, Dr. Gillian Hue and Dr. Jill Ward, for their involvement in my thesis development and evaluation. Lastly, I would like to thank my friends and family for their continuous support.

Table of Contents

List of Tables

List of Figures

Introduction

Peripheral nerve injuries (PNIs) are characterized by damage to axons and connective tissue (Menorca et al., 2013). Most commonly, peripheral nerve injuries are caused by nerve compression, crush, and transection. Besides spontaneous regeneration, the current standard of care, surgical nerve construction, has a functional recovery rate of 10% and may require extended hospitalization and rehabilitation (Juckett et al., 2022; Portincasa et al., 2007). Consequently, poor recovery from peripheral nerve injury is a significant public health concern. A non-surgical approach to treating peripheral nerve injury has not been developed, despite the slim recovery of full function in more than 200,000 new traumatic peripheral nerve injuries occurring in the US each year (Bekelis et al., 2015; Taylor et al., 2008). The reason most often ascribed to poor recovery from peripheral nerve injury is the slow and ineffective process of axon regeneration. By enhancing this process, the effectiveness of axon regeneration could be improved and heighten functional recovery.

Activity-dependent experimental treatments for PNIs, such as low-frequency (20 Hz) electrical stimulation or exercise, have been developed, but they are not viable for a significant number of individuals because of the nature of peripheral nerve injuries (Al-Majed et al., 2000; English et al., 2009; Maugeri et al., 2021; Park et al., 2019). The effectiveness of these therapies relies on the promotion of increased signaling by brain-derived neurotrophic factor (BDNF) via its tropomyosin receptor kinase B (TrkB) receptor (Gordon & English, 2016). Treatments with BDNF thus might form an alternative approach. However, its large size at 27 kDa prevents passage through the blood-brain barrier, and its short biological half-life of less than 10 minutes renders BDNF an unfeasible treatment (Wurzelmann et al., 2017). A known small-molecule BDNF mimetic, 7,8-dihydroxyflavone (7,8-DHF), signals effectively through the TrkB receptor.

It has a longer half-life of 134 minutes in plasma following 50 mg/kg oral administration and can cross the blood-brain barrier (Zhang et al., 2014). Systemic injections of 7,8-DHF following PNI did promote motor axon regeneration, but when administered orally, 7,8-DHF is rapidly inactivated (English et al., 2013). As an alternative, following oral administration, the pro-drug R13 is metabolized in the liver through an intermediary known as T1 (Figure 1) (Chen et al., 2018). T1 gradually forms 7,8-DHF, overall has a half-life of 220 minutes, and is detectable in plasma even eight hours after oral administration. This means that R13 induces prolonged TrkB signaling.

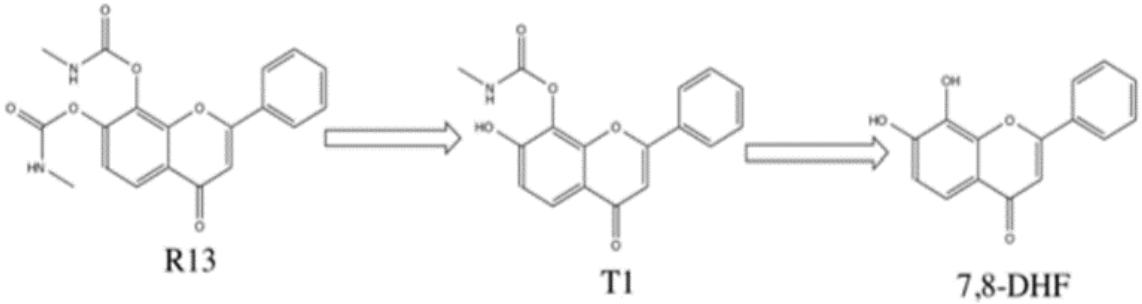

Figure 1. Hydrolysis of R13 to form 7,8-dihydroxyflavone (7,8-DHF).
Chen et al. PNAS 2018 115: 578-583

The effectiveness of oral R13 treatments on both motor and sensory axon regeneration following PNI was studied (English et al., 2022). The application of retrograde fluorescent tracers was used to mark the cell bodies of axons that successfully reinnervated skeletal muscles following sciatic nerve transection and repair in mice treated with oral R13 or vehicle. Significantly more labeled lumbar dorsal root ganglion (DRG) neurons were found in mice treated with oral R13 in comparison to vehicle-treated control mice (Figure 2A). Axons of more sensory neurons had regenerated and successfully reinnervated both the GAST and TA muscles after PNI when treated with R13. Some DRG neurons contained both retrograde fluorescent tracers and were presumed to have branched to reinnervate both muscles. However, there was no significant difference in the number of these doubly labeled neurons between the two treatment

groups studied. There was also no significant difference between treatment groups in the proportion of labeled neurons in three size classes (Figure 2B). Thus, in R13-treated mice, more sensory axons had regenerated and successfully reinnervated muscle targets than the vehicle-treated controls. Enhancements of axon regeneration due to treatments with R13 also did not bias the regeneration of axons of any one size class of DRG neuron, nor did it degrade the precision with which the regenerating axons found individual muscle targets.

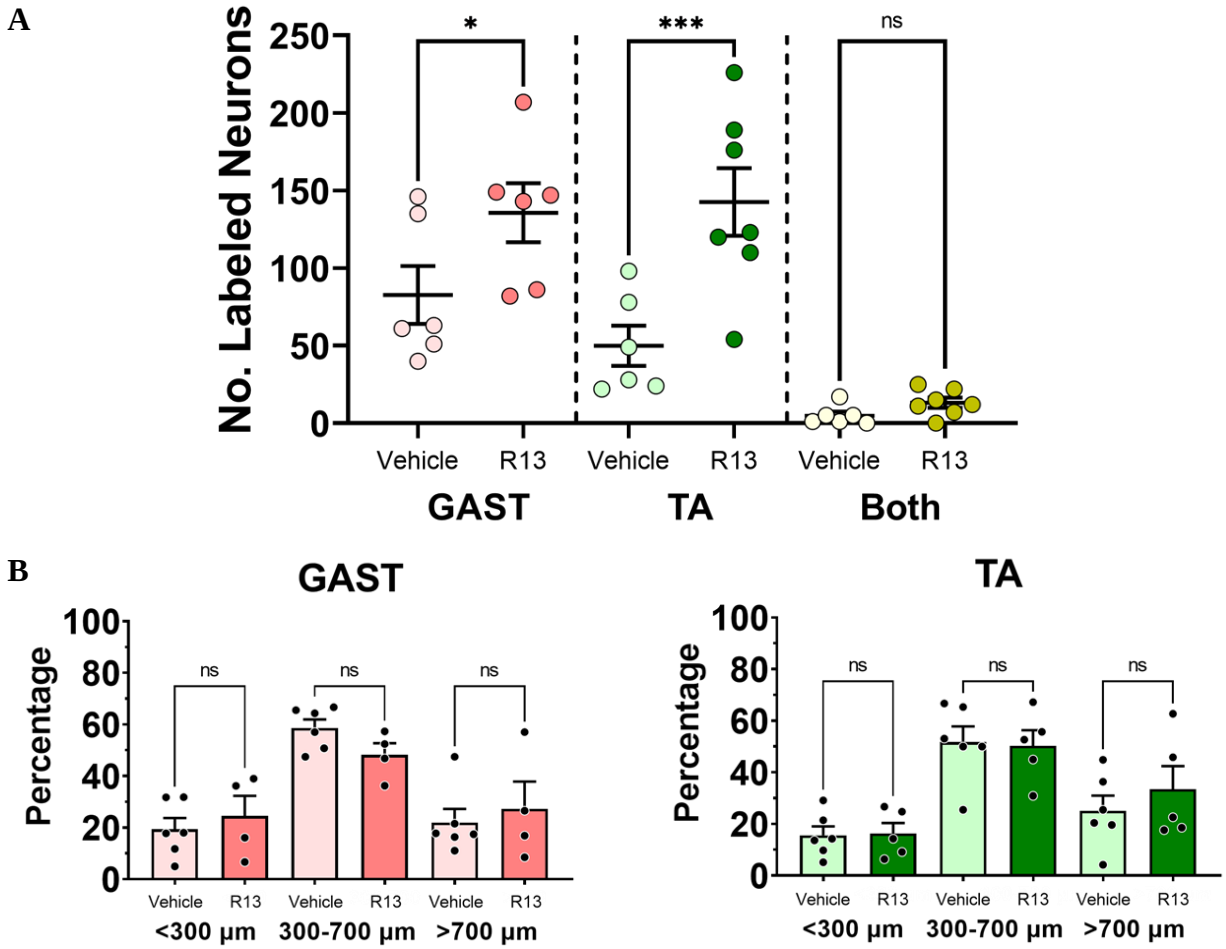

Figure 2. Analysis of mouse DRGs following treatment with R13 and vehicle-treated control. A) More labeled sensory neurons were found in R13 treated mice in GAST and TA muscles, but not in neurons innervating both muscles. B) Regeneration of large, inter-mediate, and small-sized sensory neurons was equally enhanced by R13 treatment. *=p<0.05, **=p<0.01, ***=p<0.001, ****=p<0.0001. English et al., Front. Cell. Neurosci. 16: 857664, 2022

However, whether the R13 treatments promoted the regeneration of all types of sensory axons remains unknown. A number of recent studies have demonstrated extensive cellular heterogeneity in DRG neurons and using single nucleus RNA sequencing (snRNA-seq), Renthal et al. (2020) defined nine different DRG neuron classes (Table I), each associated with a series of cell-type-specific (CTS) genes. Following peripheral nerve injury, transcription of the CTS genes was decreased, and all injured neurons started to express mRNAs for a common suite of genes, such as *Atf3* and *Sprr1a*, which are related to axon regeneration. Following successful axon regeneration after nerve crush, transcription of the CTS genes was restored. Markers for these DRG classes thus form a template for analysis of whether experimental treatments for PNI will promote the regeneration of all classes of sensory axons equally. One goal of this project was to combine retrograde labeling to assay sensory axon regeneration with immunostaining of the labeled neurons to compare the proportion of regenerated muscle afferents expressing protein markers of a selection of different classes of sensory neurons. We hypothesized that the proportions of newly successfully regenerating neurons expressing these proteins would not be changed with the administration of R13.

Table I

Dorsal Root Ganglion Neuron Classes

Class	Name	Gene Identifier*	Protein
PEP	Peptidergic Nociceptors	*Tac1*	
PEP1		*Gpx3*	TrpV1
PEP2		*Trpm8*	TrpV1
NP	Non-peptidergic nociceptors	*Mrgprd*	Isolectin B4
NF	Large Neurofilament	*Nefh*	
NF1		*Slc17a7*	VGLUT1
NF2		*Pvalb*	
NF3		*Ntrk2*	TrkB
TH	C-low threshold mechanoreceptors	*Th*	TH
SST	Somatostatin	*Nppb*	SST

Table I. Genes identified by Renthal et al. (2020) and associated proteins expressed by sensory DRG neurons.

The cellular mechanism by which R13 might act to promote axon regeneration is not fully established. It is presumed that 7,8-DHF produced by R13 metabolism acts via the TrkB receptor, but how this signaling leads to enhanced regeneration is less clear. It was recently shown that the inhibition of asparagine endopeptidase (AEP), a lysosomal cysteine protease implicated in the pathology of Alzheimer's disease, might underlie the effectiveness of R13 on axon regeneration (English et al., 2021; Zhang et al., 2014). R13 may act by metabolizing into 7,8-DHF, activating TrkB, which subsequently inhibits AEP (Wang et al., 2018). One of the known substrates of AEP is the axonal microtubule-associated protein Tau. AEP cleaves Tau at N255 and N368, thereby removing its microtubule-binding domain completely (English et al., 2021). During axon regeneration and elongation, an axonal cytoskeleton created from

microtubules helps stabilize the nascent regenerating axons (Drubin & Kirschner, 1986). These microtubules are, in turn, stabilized by Tau (Black et al., 1996). Axon regeneration is enhanced if AEP is knocked out in the regenerating axons (English et al., 2021).

Thus, the recent development of the specific AEP inhibitor, Compound 11 (CP11), as a potential therapy for Alzheimer's disease has opened the potential for its use to treat PNI. A second goal of this project was to investigate the effectiveness of treatments with CP11 on sensory axon regeneration after PNI. We hypothesized that the administration of CP11 would lead to increased sensory neuron reinnervation of muscle targets. Furthermore, the distribution of classes of DRG neurons that reinnervate these muscle and cutaneous targets after CP11 administration would not differ from the types of neurons that would normally reinnervate the targets. A comparison between the proportions of newly regenerated sensory neurons reinnervating muscle targets expressing the same protein markers as the neurons in the R13 group was made to analyze any differences in the regeneration patterns of R13- and CP11-treated mice.

Methods

Animal Surgeries – All experimental methods used were approved by the Institutional Animal Care and Use Committee of Emory University (PROTO201800101). In all experiments, C57BL/6J wild-type mice were used. To evaluate the efficacy of R13 and CP11 administration on reinnervation of muscle targets by sensory neurons, four intact, five vehicle-treated, four R13 treated, and four CP11-treated mice (all 6-12 weeks old) were studied. Intact mice did not undergo surgery, while mice in all other groups did undergo surgery. The use of intact mice allowed us to control for any change in reinnervations following surgery that could not be attributed to treatment administration. In isoflurane-anesthetized mice, the sciatic nerves were exposed in the mid-thigh, cut with sharp scissors, and immediately repaired by simple end-to-end anastomosis. Repaired nerve segments were secured in place using 6 µL of fibrin glue (Akhter et al., 2019). On the third day following surgery, mice began oral treatments with either R13 (21.8 mg/kg) or the vehicle (95% methylcellulose and 5% DMSO) in which the R13 was prepared. These R13 or vehicle treatments were repeated daily, five days per week, for two weeks. CP11-treated mice received intraperitoneal injections (10 mg/kg) daily, five days per week, for two weeks.

For all mice, four weeks after the nerve repair surgery, and two weeks after the end of treatments, the fluorescent retrograde tracers, wheat germ agglutinin (WGA), were injected into the lateral and medial heads of the gastrocnemius (GAST) muscle (WGA-555), and the tibialis anterior (TA) muscle (WGA-488). Injections were made using a Hamilton syringe with a 28G needle, with 2 µL WGA per TA muscle and 2 µL WGA per head of GAST muscle (Figure 3). These tracers were taken up and transported retrogradely to mark the somata of sensory DRG neurons that had successfully reinnervated these muscles. Three days later, the mice were

euthanized by intraperitoneal injection of Euthasol (pentobarbital sodium and phenytoin sodium, 150 mg/kg) and perfused transcardially with saline followed by 4% paraformaldehyde, pH 6.9. L4 DRGs were harvested and cryoprotected in a 20% sucrose solution at least overnight before sectioning.

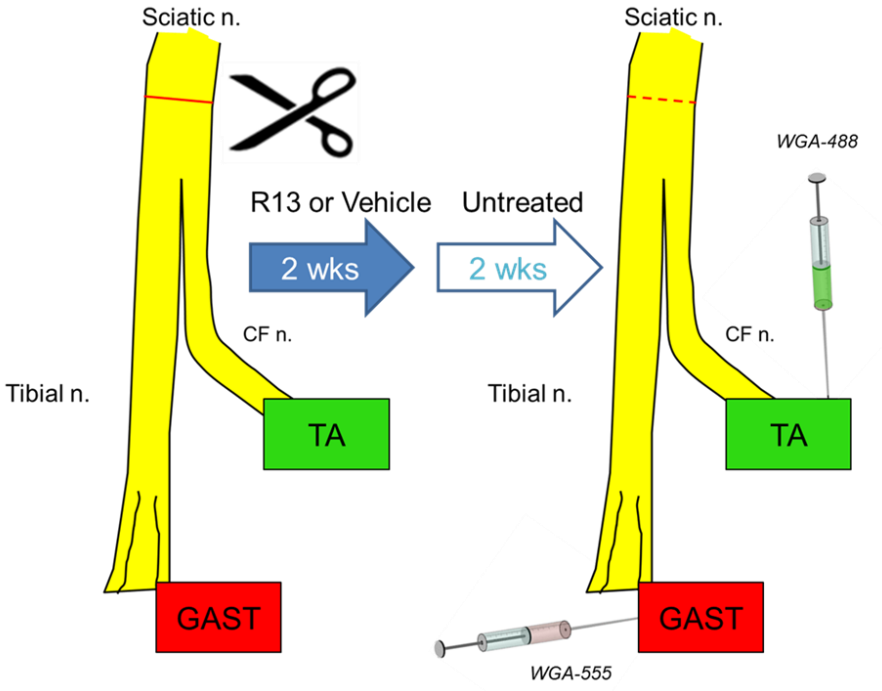

Figure 3. Animal surgery schematic. Cell bodies of sensory, dorsal root ganglion (DRG) neurons that have successfully regenerated axons and reinnervated muscle were labeled with fluorescent tracers.

Immunostaining for antibodies in regenerated sensory neurons – Cryostat sections of lumbar dorsal root ganglia, cut at 40 µm thickness, were reacted with different antibodies (Table II) to evaluate the expression of proteins associated with different classes of DRG neurons reinnervating the GAST and TA muscles. Serial DRG sections were alternately placed onto three charged glass microscope slides. To begin immunohistochemistry (IHC), a 1% phosphate-buffered saline (PBS) solution containing 10% bovine serum albumin (BSA) and 0.5% Triton was applied to all of the sections on the slides for one hour. The slides were then incubated at room temperature with primary antibodies overnight. The slides were then washed with 1% PBS

three times, and secondary antibodies were applied. Slides were incubated for two hours before being coverslipped using Vectashield®. A lectin or set of primary and secondary antibodies was used to stain each of the different proteins studied (Table II). Immunoreactivity to vesicular glutamate transporter 1 (VGLUT1) marked one subclass of Nf neurons. The binding of the antibody to the transient receptor potential cation channel subfamily V member 1 (TrpV1) was used to identify peptidergic nociceptors (PEP). The binding of Isolectin B4 (IB4) was used to identify non-peptidergic (NP) unmyelinated primary afferent neurons. Immunoreactivity to tyrosine hydroxylase (TH) marked C-low threshold mechanoreceptor afferents. Combining two antibodies on each slide with DRG neuronal sections allowed us to determine the proportion of protein expression among successfully reinnervated DRG neurons. Furthermore, this design allowed for the classification of neurons expressing proteins associated with multiple DRG neuronal types.

Table II

Immunohistochemistry - Dorsal Root Ganglion Neurons

Protein	Primary Antibody Used	Secondary Antibody/Lectin Used
TrpV1	TRPV1 Guinea Pig Anti-Human, Rat, Polyclonal, Invitrogen™ (1:100)	DyLight™ 405 AffiniPure Donkey Anti-Guinea Pig IgG (1:200)
Isolectin B4		Griffonia Simplicifolia Lectin I (GSL I) Isolectin B4, DyLight® 649 (1:200)
TH	Anti-Tyrosine Hydroxylase (1:200)	Alexafluor 405 Goat Anti-Rabbit (1:200)
VGLUT1	Anti-VGLUT1 (1:1000)	Alexafluor 647 Goat Anti-Guinea Pig (1:500)

Table II. Antibodies/lectin used for immunohistochemistry protocol and visualizing four different classes of sensory neurons in DRG. Brackets indicate antibodies stained on the same slide of DRG tissue sections.

Imaging – Images of sections were captured at 10x magnification using a Leica DM6000 upright fluorescence microscope and Hamamatsu low-light camera, using HCImage software. Sensory neurons that had regenerated successfully were identified if both the retrograde fluorescent label filled the soma and a clear nuclear region devoid of the label was present (Figure 4A). The neurons that reinnervated the GAST muscle were labeled with a red tracer (WGA-555), and the neurons that reinnervated the TA muscle were labeled with a green tracer (WGA-488). Some neurons were labeled with both tracers and appeared yellow. These cells were considered to have detected both tracers during reinnervation, and analysis for these "both" neurons was performed separately. Immunoreactivity to the proteins studied or IB4 binding was captured on the third (blue) and fourth (B&W) channels. For each of the four channels studied, the background was subtracted and the mean gray value of subjectively identified non-labeled cells was measured. For each retrogradely labeled neuron identified, the presence or absence of immunoreactivity (or IB4 binding) was determined by comparing the mean gray value to the background, or non-labeled cells, using ImageJ software. Along with the mean gray value to measure protein expression, in cells expressing retrograde labels, the soma cross-sectional area was also recorded. The proportion of reinnervated neurons expressing proteins associated with different identified classes was determined and compared between treatments.

Results

R13 and CP11 administration enhances sensory axon regeneration

Mean numbers (±SEM) of L4 DRG neurons retrogradely labeled from TA, GAST, or both muscle reinnervation, are shown for vehicle-treated, R13-treated, and CP11-treated mice in Figure 4B. In both R13- and CP11-treated mice, significantly more DRG neurons were labeled than vehicle-treated controls (ANOVA, $F_{(8,39)}=8.952$, $p<0.0001$). Using post-hoc paired testing (Benjamini, Krieger, and Yekutieli), the number of neurons reinnervating either GAST or TA were significantly greater in the R13- and CP11-treated mice, but the number of effectively regenerating neurons presumed to have detected both tracers and reinnervated both muscles following either treatment remained similar. The R13 findings corroborated those reported by English et al. (2022). Either experimental treatment nearly doubled the number of DRG neurons that regenerated and reinnervated either muscle.

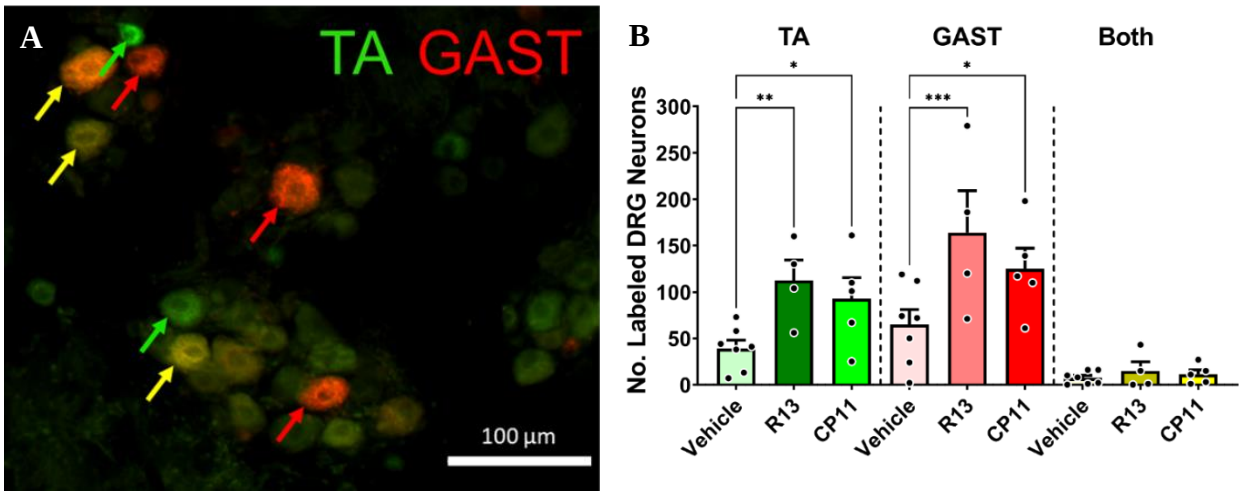

Figure 4. Analysis of mouse DRGs following treatment with vehicle-treated control, R13, and CP11. A) DRG section of a CP11-treated mouse. Cell bodies of DRG neurons which successfully reinnervated muscle targets were fluorescently labeled. Green cells reinnervated TA, while red cells reinnervated GAST. Yellow cells detected both tracers injected into either muscle. B) The average number of DRG neurons following R13 and CP11 administration was larger than vehicle-control treatment. Significant differences were found between vehicle- and R13-treated animals and vehicle- and CP11-treated animals in both the TA and GAST muscles. Only significant differences are shown. *=$p<0.05$, **=$p<0.01$, ***=$p<0.001$.

Six different phenotypes of sensory DRG neurons reinnervated the GAST and TA muscles

Retrogradely labeled sensory neurons were analyzed to determine the proportions of cells expressing protein markers associated with different classes of DRG neurons reinnervating the TA and GAST muscles. The combinations of antibodies raised in different species, indicated in Table I, made possible the identification of cells immunoreactive to VGLUT1 (NF1), TH (TH), and TrpV1 (PEP), or binding IB4 (NP).

Using this approach, six different phenotypes were found in successfully reinnervating sensory neurons of the TA and GAST muscles (Figures 5 and 9). Even though axons of many more sensory neurons regenerated successfully in the R13- or CP11-treated mice, we hypothesized that the proportions of DRG neurons in the different phenotypes would differ little between experimentally- and vehicle-treated mice. Proportions of each of these six classes, relative to all DRG neurons reinnervating TA, GAST, or presumably both muscles, were determined. The significance of differences in the proportion of labeled sensory neurons between treatment groups was evaluated in each of these phenotypes using a one-way ANOVA and post-hoc paired (Fisher's least significant difference) testing, where appropriate. Results from the different phenotypes are described in separate sections below.

Imaging of DRG neurons following immunohistochemistry for TrpV1 proteins and IB4 binding

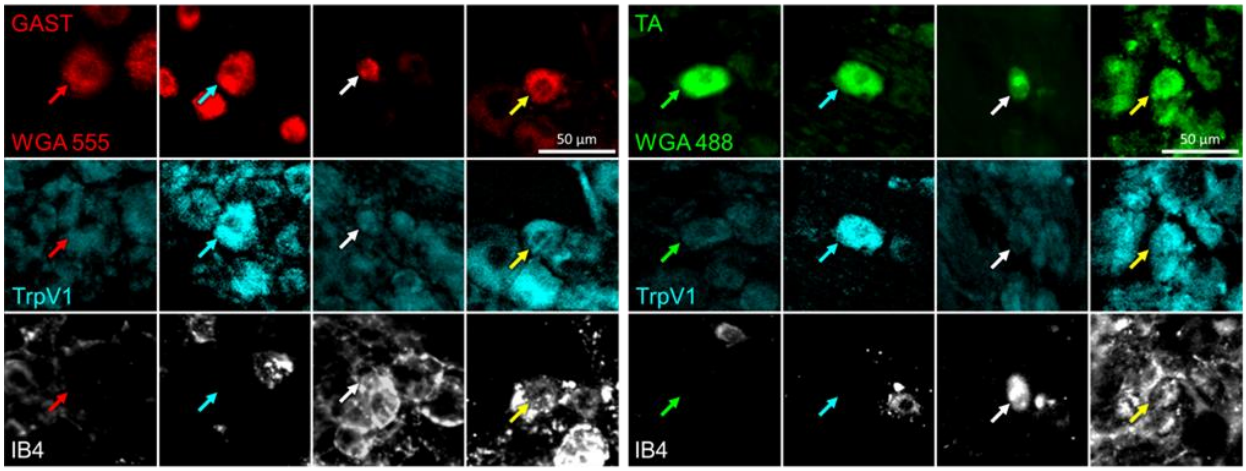

Figure 5. Example visualization of TrpV1 and IB4 staining in mouse DRGs reinnervating the TA and GAST muscles. Red arrows indicate a sensory neuron reinnervating the GAST muscle that does not express TrpV1 or bind IB4. Green arrows indicate a sensory neuron reinnervating the TA muscle that does not express TrpV1 or bind IB4. Blue arrows indicate a sensory neuron reinnervating either the GAST or TA muscle that only expresses TrpV1. White arrows indicate a sensory neuron reinnervating either the GAST or TA muscle that only binds IB4. Yellow arrows indicate a sensory neuron reinnervating either the GAST or TA muscle that both expresses TrpV1 and binds IB4.

TrpV1 – Mean (±SEM) proportions of labeled DRG neurons that were immunoreactive to TrpV1, a protein associated with peptidergic nociceptors (Figure 5), are shown in Figure 6 for intact mice and mice in the different experimental treatment groups. The percentage of TrpV1 expression did not differ greatly between treatment groups for each of the two muscles, as well as for neurons marked with both red and green tracers. In reinnervated TA muscle, a significant difference in the proportion of DRG neurons immunoreactive for TrpV1 was found (ANOVA, $F_{(3,12)}$=4.684, p=0.0218). However, based on post-hoc paired testing, the only significant difference found was the reduced proportion of neurons in all of the experimental groups relative to the intact mice. There were no significant differences among the proportions of retrogradely labeled neurons reinnervating the GAST muscle (ANOVA, $F_{(3,12)}$=0.8674, p=0.4847) and for

retrogradely labeled neurons presumed to have reinnervated both muscles (ANOVA, $F_{(3,13)}$=1.290, p=0.3194). There is overall no significant change in the proportions of neurons expressing markers associated with peptidergic nociceptors when the number of regenerating neurons is doubled following treatment with either R13 or CP11.

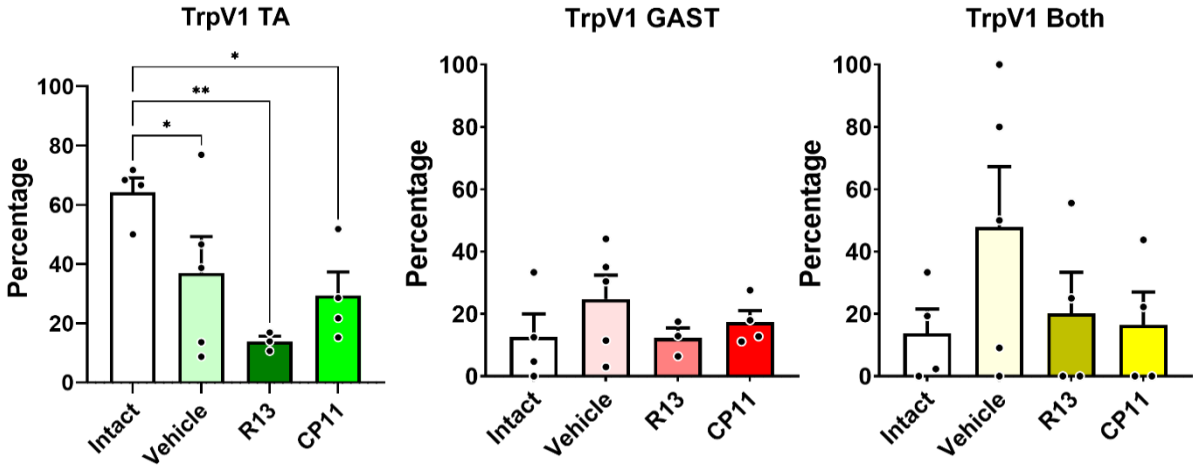

Figure 6. Analysis of TrpV1 expression in mouse DRGs in the intact condition and following treatment with vehicle-treated control, R13, or CP11. The proportion of TrpV1-expressing newly regenerated sensory neurons differed only between the intact condition and vehicle-treated, R13-treated, and CP11-treated mice in the TA muscle. Only significant differences are shown. *=p<0.05, **=p<0.01, ***=p<0.001, ****=p<0.0001.

IB4 – The binding of fluorescent Isolectin B4 was used to identify DRG neurons associated with non-peptidergic unmyelinated primary afferent neurons (Figure 5). Mean (±SEM) proportions of labeled DRG neurons that bound IB4 are shown in Figure 7 for intact mice and mice in the different experimental treatment groups. The percentage of IB4 binding neurons did not differ between intact mice and mice in the different treatment groups for each of the two muscles, as well as for neurons presumed to have reinnervated both muscles (TA (ANOVA, $F_{(3,12)}$=0.6398, p=0.6039), GAST (ANOVA, $F_{(3,13)}$=1.626, p=0.2316), and both muscles (ANOVA, $F_{(3,13)}$=1.105, p=0.3825)). There is overall no bias toward or away from the regeneration of neurons associated with non-peptidergic unmyelinated primary afferents following treatment with either R13 or CP11.

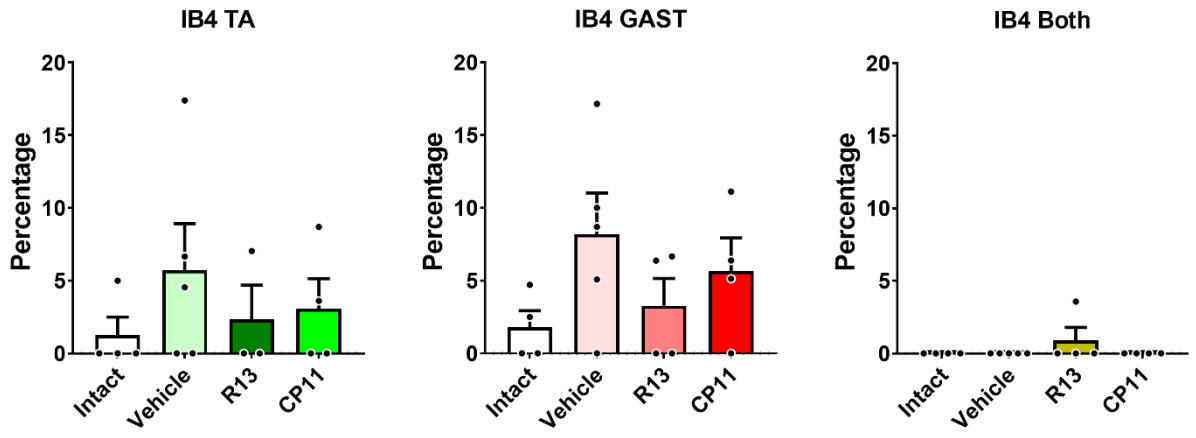

Figure 7. Analysis of IB4 binding in mouse DRGs in the intact condition and following treatment with vehicle-treated control, R13, or CP11. The proportion of IB4-expressing newly regenerated sensory neurons did not differ between the intact condition and any treatment in all muscle groups. Only significant differences are shown. *=p<0.05, **=p<0.01, ***=p<0.001, ****=p<0.0001.

TrpV1 and IB4 co-expression – During image analysis, a subset of retrogradely labeled neurons was found to be both immunoreactive for TrpV1 and bound IB4 (Figure 5) in both intact mice and in mice recovering from nerve injury. Mean (±SEM) proportions of these TrpV1/IB4 DRG neurons are shown in Figure 8 for intact mice and mice in the different experimental treatment groups. No significant differences in the percentage of TrpV1/IB4 expressing DRG neurons were found between groups treatment groups for each of the two muscles, as well as for neurons marked with red and green tracers (TA (ANOVA, $F_{(3,12)}$=0.8684, p=0.4842), GAST (ANOVA, $F_{(3,13)}$=0.8605, p=0.4860), both (ANOVA, $F_{(3,13)}$=0.6108, p=0.6199)). Thus, treatments with R13 or CP11 that dramatically increase the success of afferent axon regeneration did not result in a change in the proportion of these doubly-labeled neurons.

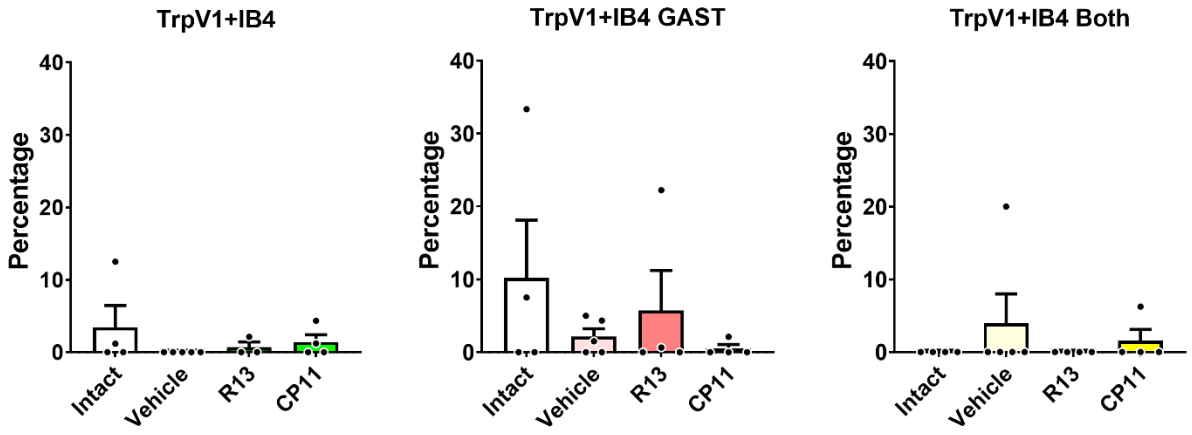

Figure 8. Analysis of TrpV1 and IB4 co-expression in mouse DRGs in the intact condition and following treatment with vehicle-treated control, R13, or CP11. The proportion of TrpV1-expressing and IB4-binding newly regenerated sensory neurons did not differ between the intact condition and any treatment in all muscle groups. Only significant differences are shown. *=p<0.05, **=p<0.01, ***=p<0.001, ****=p<0.0001.

Imaging of DRG neurons following immunohistochemistry for TH and VGLUT1 proteins

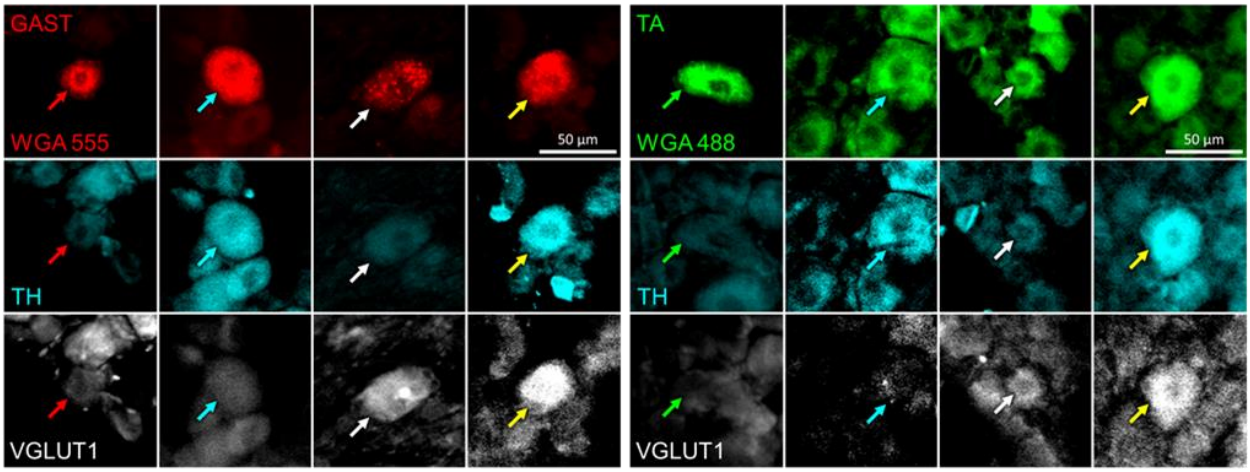

Figure 9. Example visualization of TH and VGLUT1 staining in mouse DRGs reinnervating the TA and GAST muscles. Red arrows indicate a sensory neuron reinnervating the GAST muscle that does not express TH or VGLUT1. Green arrows indicate a sensory neuron reinnervating the TA muscle that does not express TH or VGLUT1. Blue arrows indicate a sensory neuron reinnervating either the GAST or TA muscle that only expresses TH. White arrows indicate a sensory neuron reinnervating either the GAST or TA muscle that only expresses VGLUT1. Yellow arrows indicate a sensory neuron reinnervating either the GAST or TA muscle that both expresses TH and VGLUT1.

TH – Tyrosine hydroxylase (TH) immunoreactivity in intact mice is found in C-low threshold mechanoreceptors that innervate mainly skin (McGlone et al., 2014). We found that a very small proportion of larger DRG neurons retrogradely labeled from intramuscular injections of tracers were also immunoreactive for TH (Figure 9). No significant differences in the mean (±SEM) proportions of TH-expressing DRG neurons innervating the TA muscle were found (ANOVA, $F_{(3,15)}$=0.8503, p=0.4878). Significant differences were found for GAST (ANOVA, $F_{(3,16)}$=3.411, p=0.0432) and Both (ANOVA, $F_{(3,16)}$=2.118, p=0.1381). In both cohorts, a significant increase in the percentage of DRG neurons immunoreactive for TH was found in the CP11-treated animals, relative to both intact mice and the vehicle control mice, but not the R13-treated mice (Figure 10). Treatments with CP11 produce increases in the proportion of these TH immunoreactive muscle afferent neurons.

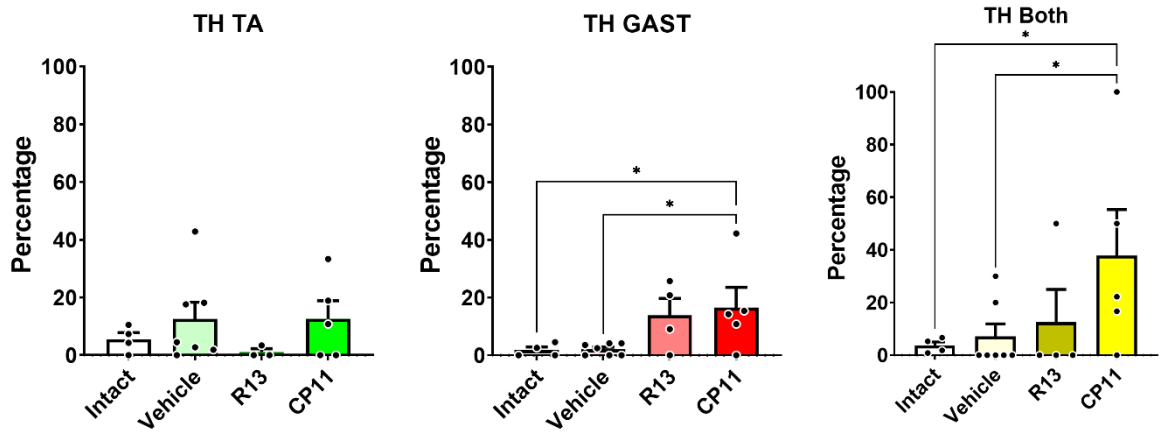

Figure 10. Analysis of TH expression in mouse DRGs in the intact condition and following treatment with vehicle-treated control, R13, or CP11. The proportion of TH-expressing newly regenerated sensory neurons differed only between the intact condition and CP11-treated mice and vehicle-treated and CP11-treated mice in the GAST muscle, and in neurons presumed to have reinnervated both muscles. Only significant differences are shown. *=p<0.05, **=p<0.01, ***=p<0.001, ****=p<0.0001.

VGLUT1 – Mean (±SEM) proportions of VGLUT1 immunoreactive DRG neurons (Figure 9) are shown in Figure 11 for intact mice and mice in the different experimental treatment groups. There were no significant differences among the proportions of retrogradely labeled neurons expressing VGLUT1 innervating the TA muscle (ANOVA, $F_{(3,14)}$=1.538, p=0.2485). Significant differences were found among proportions of retrogradely labeled neurons expressing VGLUT1 in GAST (ANOVA, $F_{(3,15)}$=13.19, p=0.0002), and Both (ANOVA, $F_{(3,14)}$=4.466, p=0.0212). In GAST and TA, treatments with R13 resulted in proportions of VGLUT1+ neurons that are similar to those found in vehicle-treated control mice.

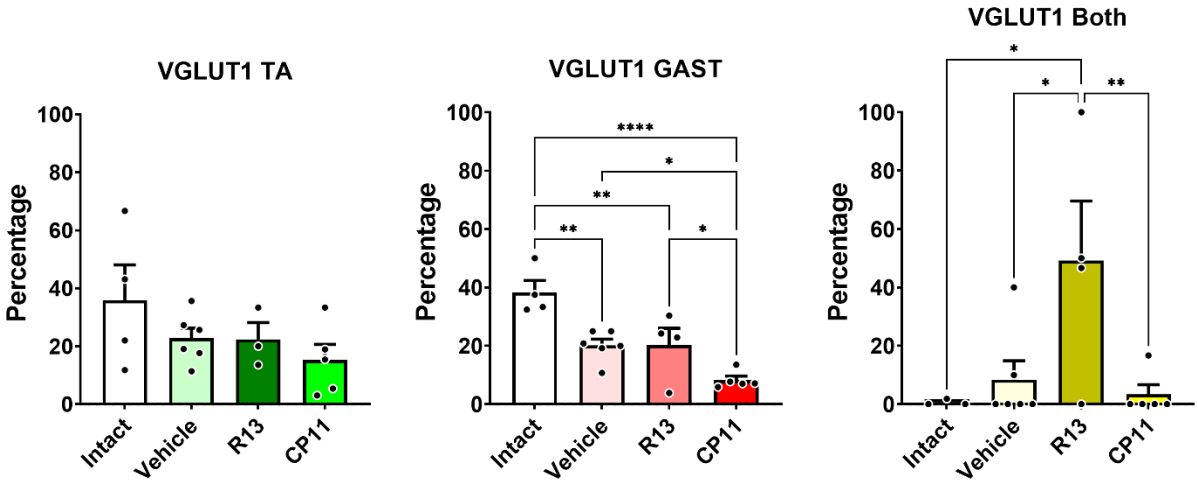

Figure 11. Analysis of VGLUT1 expression in mouse DRGs in the intact condition and following treatment with vehicle-treated control, R13, or CP11. The proportion of VGLUT1-expressing newly regenerated sensory neurons differed between the intact condition and vehicle-treated, R13-treated, and CP11-treated mice in the GAST muscle. There was also a significant difference between the vehicle-treated and CP11-treated mice, as well as the R13-treated and CP11-treated mice in reinnervation of the GAST muscle. Furthermore, the proportion of VGLUT1-expressing newly regenerated sensory neurons differed between the intact condition and R13-treated mice, between the vehicle-treated and R13-treated mice, and between R13-treated and CP11-treated mice in the neurons presumed to have reinnervated both muscles. Only significant differences are shown. *=p<0.05, **=p<0.01, ***=p<0.001, ****=p<0.0001.

TH and VGLUT1 co-expression – During analysis, a small subset of neurons was found to be immunoreactive to both TH and VGLUT1 (Figure 9). Mean (±SEM) proportions of these TH + VGLUT1 neurons are shown in Figure 12 for intact mice and mice in the different experimental treatment groups. No significant differences among the proportions of retrogradely labeled neurons expressing both TH and VGLUT1 were found for any of the muscles or treatment groups (ANOVA, $F_{(3,15)}$=1.875, p=0.1772), the GAST muscle (ANOVA, $F_{(3,16)}$=1.222, p=0.3339), and for retrogradely labeled neurons marked with both red and green tracers (ANOVA, $F_{(3,16)}$=0.1858, p=0.9045).

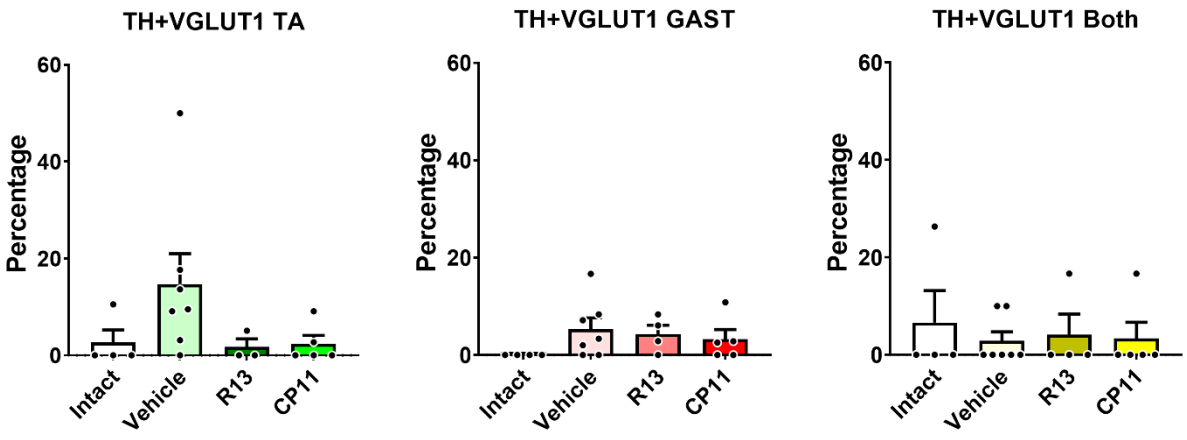

Figure 12. Analysis of TH and VGLUT1 co-expression in mouse DRGs in the intact condition and following treatment with vehicle-treated control, R13, and CP11. The proportion of TH- and VGLUT1-expressing newly regenerated sensory neurons did not differ between the intact condition and any treatment in all muscle groups. Only significant differences are shown. *=p<0.05, **=p<0.01, ***=p<0.001, ****=p<0.0001.

Overall, results are as follows:

Protein Marker(s)	***Outcome***
TrpV1	Significant reduction in proportion in TA following surgery and treatment, relative to intact, but no significant change in any of the reinnervated muscles
IB4	No significant change in any proportions
TrpV1 + IB4	No significant change in any proportions
TH	Significantly more expression following R13 and CP11 treatment in GAST and Both
VGLUT1	No effect in TA, reduction in reinnervation in GAST, and further reduction with CP11
TH + VGLUT1	No significant change in any proportions

Table III. Summary of phenotypic distributions of DRG neurons comparing the intact condition to treatment with vehicle-treated control, R13 administration, or CP11 administration.

Discussion

Poor functional recovery following peripheral nerve injuries affects thousands of patients yearly, making it a persistent public health issue. Though attempts to mediate this process have been made, through surgery, neuronal electrical activity, or exercise, a more accessible pharmacological approach has yet to be developed. Promising experimental treatments have aimed at enhancing the slow and inefficient process of axon regeneration through increased signaling through the TrkB receptor by BDNF, both directly and indirectly via increased activity in injured neurons (Gordon & English, 2016). A pharmacological approach to enhancing functional recovery following a peripheral nerve injury may overcome difficulties associated with activity-dependent treatments due to PNI patient limitations. Both R13 and CP11 are candidates for pharmacological treatment for PNI. R13 metabolizes into a BDNF-mimetic, 7,8-DHF, and signals through the TrkB receptor. CP11 targets an enzyme, AEP, that is inhibited downstream of TrkB signaling. In the current study, we aimed to investigate whether these pharmacological treatments enhance muscle sensory axon regeneration following PNI. Further, we wanted to investigate whether any enhancement with R13 or CP11 also increases the misdirection of regenerating sensory axons to muscle targets. These investigations help establish the feasibility of R13 and CP11 as pharmacological treatments following PNIs.

R13 and CP11 enhance successful reinnervation of muscle targets by sensory neurons following injury – A main finding of this study was that treatments with either R13 or CP11 resulted in the successful regeneration of axons of approximately twice as many muscle sensory neurons as vehicle-treated controls. The efficacy of R13 in enhancing sensory regeneration after nerve injury has been demonstrated previously by English et al. (2022). Using a similar

experimental design, we found here that CP11 treatments also enhanced the regeneration of muscle sensory axons and that the number of successfully regenerated sensory neurons did not significantly differ between R13 and CP11 treatments. Both R13 and CP11 should be considered promising potential pharmacological treatments to enhance the process of axon regeneration. We believe that our findings are important because current medications used in PNI patients are not directed toward nerve regeneration or acceleration, but toward the pain associated with the injury (Hussain et al., 2020). Furthermore, this finding shows that these pharmacological treatments improve upon the current standard of care, as modeled by the vehicle treatment, in which the nerve is microsurgically repaired.

Phenotypic proportions of DRG neurons are retained by reinnervated muscles following axon regeneration enhancement by R13 or CP11 – Our treatments with R13 or CP11 resulted in muscle reinnervation by sensory neurons expressing proteins associated with at least six different classes of DRG neurons. Neurons expressing these proteins were found in roughly the same proportions found in vehicle-treated controls, even though twice as many DRG neurons had reinnervated the muscles studied. This remarkable specificity of neuronal reinnervation can be explained by pathway selection, as described by Gordon & English (2016), or by target selection and reprogramming, as described by Renthal et al. (2020).

Gordon & English (2016) discuss temporally staggered regeneration, in which different regenerated axons reinnervate targets after crossing a microscopic surgical gap at different times after injury. This staggering between different neurons reinnervating targets caused a temporal delay of 8-10 weeks until all regenerating axons crossed the gap. This staggering is consistent with a potential pathway selection mechanism, especially in neurons that initiate regeneration

after a delay. Neuronal reinnervation is accelerated and this temporal gap is closed following electrical stimulation or exercise, which both involve a similar cellular pathway as R13 and similar inhibition of AEP as with CP11. Bolívar, et al. (2020) suggested that trophic factors, target contact, or potentially, repair Schwann cells that express certain markers that are retained even after regeneration, can influence how motor neurons and sensory neurons might select pathways leading to specific targets. Brushart (1993) first proposed that specific Schwann cell markers associated with pathways might lead regenerating axons selectively to muscle or cutaneous targets. Similarly, Schwann cell markers could also potentially lead to specificity in the selection of regeneration pathways by different classes of sensory neurons. The net result would be consistent with the results presented above.

An alternative explanation for the specificity in reinnervation patterns between muscles and between phenotypes could stem from the transcriptional reprogramming in DRG neurons following a nerve injury, as described by Renthal et al. (2020) using a crush model. Though spontaneous nerve regeneration is random, there is neuronal reprogramming during the regeneration process. Neurons enter a transcriptional state and express a common suite of genes associated with an “injured state,” associated with axon regeneration, but this also suppresses the cell’s identity. Once axon regeneration is successful, the cell-type-specific genes are re-expressed. This reprogramming of the cell could align with its previous identity through signaling from the target or a specific pathway, either of which would involve a retrograde signal to prompt the neuron to express a certain, possibly novel, set of protein markers. Reprogramming in response to these signals would result in the successful regeneration of sensory neuronal classes regardless of treatment, as generally seen in our results. The possibility of such a

retrograde signal could be tested by using both muscle and non-muscle, such as cutaneous, targets and analyzing the expression of neurons associated with DRG phenotypes.

Though pathway and endoneurial tube selection at the injury site according to its previous identity by regenerating axons could be a potential mechanism for neuronal regeneration specificity, a marked decrease in temporal staggering was found with both experimental treatments, above. This more synchronous initiation of axon regeneration would leave less time for pathway selection. Thus, target selection and reprogramming are a more likely mechanism to explain the regeneration specificity observed within this study. However, some of the specificity of muscle sensory reinnervation observed here may involve both of our proposed mechanisms. Further study into distinguishing the mechanism involved in this specificity is necessary to understand how our experimental treatments can non-specifically enhance the regeneration of sensory neurons following PNI.

Exceptions were found in comparing protein expression in regenerated neurons and class association – Differences were found in neurons reinnervating the TA muscle expressing TrpV1 markers, as an overall reduction in these neurons was found after surgery. Nevertheless, a significant difference was not found between treatment groups, so the reduction may be common to all regenerating sensory axons reinnervating that muscle. An increase in the proportion of neurons reinnervating the GAST and presumably both muscles expressing TH markers, and a decrease in the proportion of neurons reinnervating the GAST and both muscles expressing VGLUT1 markers were also found. A possible explanation of the differential distribution between phenotypes may be that reprogramming of these neurons following injury may be slower, though this is unlikely because of the similarity in proportions between the vehicle and

experimental treatments in comparison to the intact condition. Instead, TH- and VGLUT1-expressing neurons may represent the limitations of reprogramming. The mechanism prompting the reprogramming of cells may be less effective in prompting protein marker expression in these classes of DRG neurons than it is in smaller TrpV1-expressing and IB4-binding neurons. Doubly-labeled neurons expressing more than one kind of protein marker, such as both TrpV1 and IB4 or both TH and VGLUT1, were also found. However, there was no significant difference in the presence of doubly-labeled neurons among the treatment groups, and very few doubly-labeled neurons were successfully regenerated, so a similar process is involved regardless of condition or treatment.

Limitations to this study – When analyzing microscope images from intact animals, a very small number of cells that had seemed to reinnervated both muscles were present. We had originally interpreted these doubly innervated neurons to be regenerating axons that had branched to reinnervate both muscles following nerve injury. Yet intact mice, which received no nerve injury, contained some doubly innervated cells. Neurons could be labeled in yellow because they branched and innervated both muscles or the growing neuron could have detected both tracers. Ultimately, there was no significant difference in the number of doubly-labeled cells among treatment groups, but the results of analyses of "both" should be considered with this limitation.

Another limitation of this experimental design is the difference in treatment delivery method. R13 was administered orally, and control mice in this cohort were also given the vehicle orally. However, CP11 was administered through intraperitoneal injection, and control mice in this cohort were also given vehicle via intraperitoneal injection. Though we do not expect the

delivery method to have a large influence on the degree of successful muscular reinnervation by sensory axons, this difference in delivery may be a confounding variable when comparing the efficacies of R13 and CP11. Data from oral treatment with CP11 are currently being collected. Intraperitoneal injection of CP11 lacks clinical relevance when compared to oral administration of the drug. Consequently, the demonstrated effectiveness of CP11 should be considered with this in mind. The oral administration of CP11 and its effects on the number of successfully reinnervated sensory neurons, along with the phenotypic distribution of sensory neurons in the DRG, will be analyzed in the future.

Other limitations that may be considered are the inconsistency in some antibodies used throughout the procedure and the IHC design. There was a change in the TrpV1 antibody used between intact mice and CP11-treated mice. Though a newer antibody was used for the CP11 cohort of mice, this discrepancy may have influenced TrpV1 neuronal counts and identification in intact mice, for which the previous antibody was used. Additionally, because slides were only analyzed for either TrpV1/IB4 or TH/VGLUT1, there may be combinations of these antibodies that were not used that may reveal other subsets of doubly-labeled cells, such as cells expressing both TrpV1 and TH.

In the future, an analysis of cutaneous rather than muscle tissue should be made to determine the consistency and ability of sensory neurons to successfully reinnervate targets. Furthermore, English et al. (2022) showed R13's effects on both sensory neurons in the DRG, as well as motoneurons in the spinal cord. Another future direction is to classify the types of motoneurons (alpha and gamma motoneurons) and the distribution of these classes following R13 and CP11 administration, if feasible, and to investigate neuronal distributions at a longer timepoint past the

four weeks seen in this study. Overall, this study contributed to our current scientific understanding of PNIs by elucidating a possible mechanism by which sensory axons regenerate. Our study showed that both R13 and CP11 are pharmacological approaches to PNI that do enhance axon regeneration, and led to a clearer understanding of any biases in neuronal regeneration that may arise following treatment.

Overall, both R13 and CP11 enhanced the successful reinnervation of muscle targets by sensory neurons following a PNI in mice. Establishing the efficacy of both of these pharmacological targets allows for further research into developing a more accessible and reliable therapy for PNI, as an alternative to a surgical or activity-based approach. By classifying the phenotypic profiles of successfully regenerated sensory neurons, we have found that little bias exists in these neurons in comparison to the current standard of care, and both R13 and CP11 remain potential candidates as PNI therapeutics. Further investigation into both R13 and CP11 in the pathways used for enhanced axon regeneration as an explanation for the variable differences across phenotypes and between treatments is necessary. Investigation into the efficacy of CP11 via oral administration, as it is a more clinically relevant delivery method of this pharmacological treatment, is also necessary. R13 and CP11 are both promising drug-based approaches to enhancing axon regeneration and function and in turn, quality of life, for individuals living with PNI.

Bibliography

Akhter, E. T., Rotterman, T. M., English, A. W., & Alvarez, F. J. (2019). Sciatic Nerve Cut and Repair Using Fibrin Glue in Adult Mice. *Bio Protoc*, *9*(18). https://doi.org/10.21769/BioProtoc.3363

Al-Majed, A. A., Neumann, C. M., Brushart, T. M., & Gordon, T. (2000). Brief electrical stimulation promotes the speed and accuracy of motor axonal regeneration. *J Neurosci*, *20*(7), 2602-2608. https://doi.org/10.1523/JNEUROSCI.20-07-02602.2000

Bekelis, K., Missios, S., & Spinner, R. J. (2015). Falls and peripheral nerve injuries: an age-dependent relationship. *J Neurosurg*, *123*(5), 1223-1229. https://doi.org/10.3171/2014.11.JNS142111

Black, M. M., Slaughter, T., Moshiach, S., Obrocka, M., & Fischer, I. (1996). Tau is enriched on dynamic microtubules in the distal region of growing axons. *J Neurosci*, *16*(11), 3601-3619. https://doi.org/10.1523/JNEUROSCI.16-11-03601.1996

Bolivar, S., Navarro, X., & Udina, E. (2020). Schwann Cell Role in Selectivity of Nerve Regeneration. *Cells*, *9*(9). https://doi.org/10.3390/cells9092131

Brushart, T. M. (1993). Motor axons preferentially reinnervate motor pathways. *J Neurosci*, *13*(6), 2730-2738. https://doi.org/10.1523/JNEUROSCI.13-06-02730.1993

Chen, C., Wang, Z., Zhang, Z., Liu, X., Kang, S. S., Zhang, Y., & Ye, K. (2018). The prodrug of 7,8-dihydroxyflavone development and therapeutic efficacy for treating Alzheimer's disease. *Proc Natl Acad Sci U S A*, *115*(3), 578-583. https://doi.org/10.1073/pnas.1718683115

Dall, E., & Brandstetter, H. (2013). Mechanistic and structural studies on legumain explain its zymogenicity, distinct activation pathways, and regulation. *Proc Natl Acad Sci U S A*, *110*(27), 10940-10945. https://doi.org/10.1073/pnas.1300686110

Drubin, D. G., & Kirschner, M. W. (1986). Tau protein function in living cells. *J Cell Biol*, *103*(6 Pt 2), 2739-2746. https://doi.org/10.1083/jcb.103.6.2739

English, A. W., Carrasco, D., Hoffman, D., Isaacson, R., Kang, S. S., Khan, S., Liu, X., & Ye, K. (2022). Oral Treatments With the TrkB Ligand Prodrug, R13, Promote Enhanced Axon Regeneration Following Peripheral Nerve Injury. *Front Cell Neurosci*, *16*, 857664. https://doi.org/10.3389/fncel.2022.857664

English, A. W., Cucoranu, D., Mulligan, A., & Sabatier, M. (2009). Treadmill training enhances axon regeneration in injured mouse peripheral nerves without increased loss of topographic specificity. *J Comp Neurol*, *517*(2), 245-255. https://doi.org/10.1002/cne.22149

English, A. W., Liu, K., Nicolini, J. M., Mulligan, A. M., & Ye, K. (2013). Small-molecule trkB agonists promote axon regeneration in cut peripheral nerves. *Proc Natl Acad Sci U S A*, *110*(40), 16217-16222. https://doi.org/10.1073/pnas.1303646110

English, A. W., Liu, X., Mistretta, O. C., Ward, P. J., & Ye, K. (2021). Asparagine Endopeptidase (delta Secretase), an Enzyme Implicated in Alzheimer's Disease Pathology, Is an Inhibitor of Axon Regeneration in Peripheral Nerves. *eNeuro*, *8*(1). https://doi.org/10.1523/ENEURO.0155-20.2020

Gordon, T., & English, A. W. (2016). Strategies to promote peripheral nerve regeneration: electrical stimulation and/or exercise. *Eur J Neurosci*, *43*(3), 336-350. https://doi.org/10.1111/ejn.13005

Hussain, G., Wang, J., Rasul, A., Anwar, H., Qasim, M., Zafar, S., Aziz, N., Razzaq, A., Hussain, R., de Aguilar, J. G., & Sun, T. (2020). Current Status of Therapeutic Approaches against Peripheral Nerve Injuries: A Detailed Story from Injury to Recovery. *Int J Biol Sci*, *16*(1), 116-134. https://doi.org/10.7150/ijbs.35653

Juckett, L., Saffari, T. M., Ormseth, B., Senger, J. L., & Moore, A. M. (2022). The Effect of Electrical Stimulation on Nerve Regeneration Following Peripheral Nerve Injury. *Biomolecules*, *12*(12). https://doi.org/10.3390/biom12121856

Maugeri, G., D'Agata, V., Trovato, B., Roggio, F., Castorina, A., Vecchio, M., Di Rosa, M., & Musumeci, G. (2021). The role of exercise on peripheral nerve regeneration: from animal model to clinical application. *Heliyon*, *7*(11), e08281. https://doi.org/10.1016/j.heliyon.2021.e08281

McGlone, F., Wessberg, J., & Olausson, H. (2014). Discriminative and affective touch: sensing and feeling. *Neuron*, *82*(4), 737-755. https://doi.org/10.1016/j.neuron.2014.05.001

Menorca, R. M., Fussell, T. S., & Elfar, J. C. (2013). Nerve physiology: mechanisms of injury and recovery. *Hand Clin*, *29*(3), 317-330. https://doi.org/10.1016/j.hcl.2013.04.002

Park, S., Liu, C. Y., Ward, P. J., Jaiswal, P. B., & English, A. W. (2019). Effects of Repeated 20-Hz Electrical Stimulation on Functional Recovery Following Peripheral Nerve Injury. *Neurorehabil Neural Repair*, *33*(9), 775-784. https://doi.org/10.1177/1545968319862563

Portincasa, A., Gozzo, G., Parisi, D., Annacontini, L., Campanale, A., Basso, G., & Maiorella, A. (2007). Microsurgical treatment of injury to peripheral nerves in upper and lower limbs: a critical review of the last 8 years. *Microsurgery*, *27*(5), 455-462. https://doi.org/10.1002/micr.20382

Renthal, W., Tochitsky, I., Yang, L., Cheng, Y. C., Li, E., Kawaguchi, R., Geschwind, D. H., & Woolf, C. J. (2020). Transcriptional Reprogramming of Distinct Peripheral Sensory Neuron Subtypes after Axonal Injury. *Neuron*, *108*(1), 128-144 e129. https://doi.org/10.1016/j.neuron.2020.07.026

Rotterman, T. M., Akhter, E. T., Lane, A. R., MacPherson, K. P., Garcia, V. V., Tansey, M. G., & Alvarez, F. J. (2019). Spinal Motor Circuit Synaptic Plasticity after Peripheral Nerve Injury Depends on Microglia Activation and a CCR2 Mechanism. *J Neurosci*, *39*(18), 3412-3433. https://doi.org/10.1523/JNEUROSCI.2945-17.2019

Taylor, C. A., Braza, D., Rice, J. B., & Dillingham, T. (2008). The incidence of peripheral nerve injury in extremity trauma. *Am J Phys Med Rehabil*, *87*(5), 381-385. https://doi.org/10.1097/PHM.0b013e31815e6370

Wang, Z. H., Wu, W., Kang, S. S., Liu, X., Wu, Z., Peng, J., Yu, S. P., Manfredsson, F. P., Sandoval, I. M., Liu, X., Wang, J. Z., & Ye, K. (2018). BDNF inhibits neurodegenerative disease-associated asparaginyl endopeptidase activity via phosphorylation by AKT. *JCI Insight*, *3*(16). https://doi.org/10.1172/jci.insight.99007

Wurzelmann, M., Romeika, J., & Sun, D. (2017). Therapeutic potential of brain-derived neurotrophic factor (BDNF) and a small molecular mimics of BDNF for traumatic brain injury. *Neural Regen Res*, *12*(1), 7-12. https://doi.org/10.4103/1673-5374.198964

Zhang, Z., Song, M., Liu, X., Kang, S. S., Kwon, I. S., Duong, D. M., Seyfried, N. T., Hu, W. T., Liu, Z., Wang, J. Z., Cheng, L., Sun, Y. E., Yu, S. P., Levey, A. I., & Ye, K. (2014). Cleavage of tau by asparagine endopeptidase mediates the neurofibrillary pathology in Alzheimer's disease. *Nat Med*, *20*(11), 1254-1262. https://doi.org/10.1038/nm.3700